Simulation of the Influence of Residential Biomass Burning on Air Quality in an Urban Area

Evangelia Siouti[1,2], Konstantinos Kilafis[1], Ioannis Kioutsioukis[3], Spyros N. Pandis[1,2]

[1]Department of Chemical Engineering, University of Patras, Patras, Greece
[2]Institute of Chemical Engineering Sciences (ICE-HT), Foundation for Research and Technology Hellas (FORTH), Patras, Greece
[3]Department of Physics, University of Patras, Patras, Greece

Abstract

Residential biomass burning is often one of the dominant local sources of air pollution in urban areas during the winter months. However, the corresponding particle emissions are quite uncertain and chemical transport models (CTMs) often have difficulties reproducing the observed winter particulate matter (PM) concentrations. In this work, we combine measurements from a low-cost PM sensor network and the CTM PMCAMx (Particulate Matter Comprehensive Air quality Modeling with extensions) to estimate the spatial and temporal distribution of biomass burning emissions in an urban area.

An estimate of 8100 kg d^{-1} (40 g d^{-1} per person) $PM_{2.5}$ emissions from residential biomass burning was calculated for the city of Patras including organic compounds with effective saturation concentrations C^* up to 10^4 μg m^{-3}. The spatial distribution of the emissions was based on the density of fireplaces in the city. The temporal distribution of emissions was based on measurements of the biomass burning organic aerosol (bbOA) and are higher from 18:00 to 22:00 LT peaking at 21:00 LT. The nighttime (18:00-22:00 LT) bbOA emissions were 4 times higher than the corresponding morning (8:00-13:00 LT) ones. Estimated biomass burning emissions vary from day to day based on ambient temperature, with higher emissions during the colder days. The Volatility Basis Set (VBS) was used to simulate bbOA that is treated as semi-volatile and chemically reactive.

PMCAMx predicts that bbOA concentration reaches on average 15 μg m^{-3} in the high-density bbOA emission area during the simulated period, while the

corresponding peak hourly concentrations are higher than 40 μg m^{-3} most of the nights. The average predicted bbOA concentration in the city center is 3-6 μg m^{-3} and is lower than 1 μg m^{-3} at the suburbs. The model predicts that bbOA concentrations peak at 9:00 LT in the morning and at 21:00 LT during the nighttime, reproducing the bbOA measurements.

1. Introduction

$PM_{2.5}$ (PM with a diameter lower than 2.5 μm) has major impacts on human health causing premature deaths, heart, and lung diseases, but also reduces visibility, and can damage ecosystems (Xing et al., 2016; Hayes et al., 2020; EPA 2022). Organic aerosol (OA) accounts for more than 50% of fine PM in urban areas (Kanakidou et al., 2005) and is emitted either directly from sources (primary) or can be produced in the atmosphere through gas-to-particle conversion processes (secondary). Major OA sources include transportation, industry, cooking, and residential biomass burning.

Biomass burning for heating purposes is the predominant source of air pollution in a lot of European urban areas during winter and especially during nighttime (Alfarra et al., 2007; Puxbaum et al., 2007; Akagi et al., 2011; Pikridas et al., 2013). Fuller et al. (2013; 2014) reported that wood burning was the most important source of PM_{10} in London, Paris, and Berlin during winter 2009-2011. In Paris, bbOA accounted for 33% of the total OA on average, with high contributions during the nighttime (Crippa et al., 2013a; 2013b). In Greece, Florou et al. (2017) reported that bbOA was the main component of OA during winter and especially in the evenings. In Athens, the contribution of bbOA to the total OA was around 45%, while in Patras 60%. For Athens in particular, as much as 90% of OA during the winter nights was due to biomass burning, with extremely high concentrations during cold, calm periods without rain (Kalogridis et al., 2018). Studies in Ioannina (Sindosi et al., 2019), Kavala and Drama (Gaidajis et al., 2014) indicated similar results with high PM concentrations due to biomass burning from early in the afternoon until late in the evening.

There have been a number of efforts to simulate the influence of residential biomass burning. Tian et al. (2009) used the Community Multiscale Air Quality (CMAQ) CTM to investigate the contributions of different biomass burning sources in Atlanta. During January 2002, primary OA from residential heating contributed approximately 30% of the total POA, while POA dominated the concentrations of biomass burning $PM_{2.5}$. Burr and Zhang (2011) using the CMAQ model over the eastern U.S. at 12 km resolution found that during the wintertime biomass burning was the dominant source of pollution with a contribution to $PM_{2.5}$ of 14% on average. Hu et al. (2014) combined a source apportionment method and a CTM to show that during winter biomass burning is the most important $PM_{2.5}$ source for several US cities. Athanasopoulou et al. (2017) applied the COnsortium for SMall-scale Modeling-Aerosols and Reactive Trace gases (COSMO-ART) model in Athens with a 0.025 x 0.025° (around 3 x 3 km^2) spatial resolution. They predicted that during smog periods, 80% of OA comes from residential biomass burning. Fountoukis et al. (2014) predicted a contribution of 30-60% of bbOA to primary OA (POA) on average in Europe using the PMCAMx/PSAT model. Theodoritsi and Pandis (2019) used the source-resolved version of PMCAMx (PMCAMx-SR) and estimated that bbOA (include wildfires, residential and agriculture waste burning) contributed 47% to total OA on average in Europe during the wintertime.

Most of primary bbOA is semivolatile and can evaporate in ambient conditions (Lipsky and Robinson, 2006; Cappa and Jimenez, 2010; Hennigan et al., 2011; May et al., 2015). However, a lot of studies treat bbOA as non-volatile and chemically inert (Tian et al., 2009; Burr and Zhang, 2011; Hu et al., 2014). Grieshop et al. (2009) measured the volatility distribution of OA emissions from a wood stove, while Cappa and Jimenez (2010) estimated the volatility of ambient bbOA based on their measurements. Dilution and thermodenuder measurements were used by May et al. (2013) to estimate the volatility distribution of bbOA.

The estimation of residential bbOA emissions is challenging due to their dependence on temperature, space and time. Athanasopoulou et al. (2017) used the TNO-MACC II emission inventory for residential biomass burning emissions with an updated temporal profile consistent with the Greek habits, but their spatial resolution was relatively coarse (0.125^o x 0.0625^o) and there was no temperature dependance. Xing et al. (2018) estimated the emissions from domestic biomass burning based on fuel consumption. The spatial resolution used was also high (0.25^o x 0.25^o) and the corresponding emissions were not dependent on temperature.

In this study, we investigate the effects of wintertime biomass burning on PM levels in the city of Patras, Greece. More specifically, we combine a state-of-the-art chemical transport model, PMCAMx, at a high spatial resolution of 1x1 km^2, with ambient measurements to estimate the biomass burning particulate emissions, their spatial and temporal profiles, their variation from day to day, and their effect on local air quality during wintertime at different parts in the city. This methodology can be applied to other urban areas to constrain this important air pollution source.

2. Model description

PMCAMx v2.0 (Fountoukis et al., 2011) is the research version of CAMx (ENVIRON, 2003) and simulates the physical and chemical processes that take place in the atmosphere. The model simulates air pollutant emissions, horizontal and vertical dispersion, horizontal and vertical advection, gas, aqueous and aerosol chemistry, aerosol dynamics, and wet and dry deposition by solving the continuity equation for pollutants at each time step (ENVIRON, 2003). For gas-phase chemistry, the extended Statewide Air Pollution Research Center (SAPRC) mechanism (Carter, 2000; ENVIRON, 2003) is used, which includes 217 reactions and 114 species. For aqueous-phase chemistry, the Variable Size Resolution Model (Fahey and Pandis, 2001) is employed. The partitioning of inorganic aerosol components between the gas and particulate phases is simulated using the ISORROPIA thermodynamic model (Nenes et al., 1998; 1999). A scavenging model for aerosol and gases is used for simulating wet deposition (Seinfeld and Pandis, 2006), while the dry deposition simulation is based on the approach of Wesely (1989) and Slinn and Slinn (1980). Coagulation of aerosol particles is modelled using the approach of Tambour and Seinfeld (1980).

The model treats both primary and secondary organic aerosol as semivolatile and chemically reactive using the 1-D VBS for their simulation (Donahue et al., 2006; Fountoukis et al., 2014). The organic compounds are divided into logarithmically spaced volatility bins according to their effective saturation concentration C^* at 298 K. Low-volatility organic compounds (LVOCs) are always found in the particle phase with 3.2×10^{-4} μg m^{-3} < C^*< 0.32 μg m^{-3}, intermediate-volatility organic compounds (IVOCs) are always in the gas phase with 320 μg m^{-3} < C^*< 3.2×10^{6} μg m^{-3} and semi-volatility organic compounds (SVOCs) are found both in particle and gas phase and have 0.32 μg m^{-3} < C^*< 320 μg m^{-3} (Murphy et. al., 2014). The simulation of condensation and evaporation is based on the Gaydos et al. (2003) approach.

2.1 Meteorology

The Weather Research and Forecasting (WRF) model v4.1.5 was applied for December 2021 to produce the necessary meteorological data for PMCAMx (Skamarock et al., 2008). The WRF configuration used four two-way nests, dynamically downscaling the meteorological information from a high-resolution domain of 36x36 km^2 to a fine domain over the city of Patras with a high resolution of 1x1 km^2 using 4 grids with 36x36, 12x12, 3x3 and 1x1 km^2 resolution. In the vertical, 28 sigma levels are used extending up to a height of approximately 20 km. Initial and boundary conditions for WRF are generated from the Global Forecasting System (GFS). More details can be found in Siouti et al. (2022).

2.2 PM source-apportionment algorithm

The PSAT (Particulate Source Apportionment Technology) algorithm was applied in parallel with PMCAMx to predict the sources of pollutants for the simulation period (Skyllakou et al., 2017). In this application, the algorithm tracked separately the sources of residential biomass burning, road transport, cooking, marine, ships, biogenic, other sources, long-range transport and initial conditions. More details can be found in Siouti et al. (2022).

3. Model application

PMCAMx was applied over Europe focusing on the urban area of Patras through multiple grids with increasing spatial resolution. Boundary conditions for the outer European domain were generated using the Mozart-4 model (Emmons et al., 2010). The European domain has a horizontal spatial resolution of 36x36 km^2 and the simulated urban domain has a resolution of 1x1 km^2 (Fig. 1). The outer European domain covers a region of 5400x5832 km^2, while the inner urban domain a region of 36x36 km^2. In the vertical, there are 14 layers up to 6 km for all the modelling domains. The ground layer has a height of around 50 m. The period of simulation is a winter month (December 2021), when the contribution of wood burning in fireplaces to air pollution in the urban area is expected to be high. The multigrid system used in this study allows the simulation of the formation of SOA and other secondary aerosol components in all domains and of course in the coarse resolution domain over Europe. Therefore, the model directly simulates the regional transport of SOA from other cities and areas to the city of Patras.

3.1 Emissions by other sources

Emissions by other sources besides residential biomass burning are also included in the model application. These emissions are anthropogenic (industry, domestic processes, road and non-road transport, mining, agriculture, cooking), biogenic and marine. The emissions of Siouti et al. (2021) are used in this work.

3.2 Estimation of total biomass burning PM emissions

The city of Patras includes 80330 households according to the latest available census (Hellenic Statistical Authority, 2011). In Greece, 7.4% of households use fireplaces as a primary heating source, while an additional 27.5% use them as a secondary source (Papada and Kaliampakos, 2017). Assuming that the same ratios are applicable for Patras, we estimate 28000 fireplaces in the city. A widely used wood type in traditional heating devices in southern Greece is olive wood (Florou et al., 2017). Approximately, 7.8 kg h^{-1} of olive wood is burned in traditional Mediterranean fireplaces (Castro et al., 2018; Sornek et al., 2017; Vu et al., 2012). Assuming that the fireplaces are used on average for 5 h per day based on the bbOA measurements of Florou et al. (2017) in Patras, we estimate a wood burning rate of 39 kg d^{-1} of fuel per house. Assuming a PM emission rate of 7.5 g kg^{-1} for olive wood (Gonçalves et al., 2012; Kostenidou et al., 2013.; Alves et al., 2011), we estimate that the total average PM emissions from wood burning in fireplaces in Patras are 8100 kg d^{-1}. These emissions cover the volatility range up to $C^{*}=10^{4}$ μg m^{-3} at 298 K, so they include low volatility, semivolatile and even some intermediate volatility organic compounds.

3.2.1 Spatial distribution

The estimated bbOA emissions correspond to 70 kg d^{-1} km^{-2} assuming a uniform spatial distribution for the urban/suburban and background areas in the modeling domain. The urban, suburban and background areas of Patras are shown in Figure 1c. To improve upon this rough initial estimate, the populated area was divided into regions, based on their individual characteristics. The southern part of the city has the highest density of fireplaces in the corresponding apartments because they are newer and the new construction in Greece includes fireplaces. We estimated that the emission rate is 6 times higher than the average in this region, corresponding to 420 kg d^{-1} km^{-2}. The northern/central part of Patras older construction and is characterized by low density of population and fireplaces and therefore lower wood burning emissions. The emissions were estimated to be 40% less than the average in this region and equal to 42 kg d^{-1} km^{-2}. Finally, in the outer suburbs, there is much lower population density and there are few sources of residential biomass burning, thus we assume a rate of 90% lower than the average and equal to 7 kg d^{-1} km^{-2}. These values were initially estimated based on the population density of these areas and then were improved by successive simulations comparing the $PM_{2.5}$ model predictions with the corresponding low-cost sensor measurements. The spatial distribution of those emissions is shown in Figure 2.

3.2.2 Diurnal variation

We assumed that bbOA emissions are mostly during the nighttime and in the morning. Florou et al. (2017) have measured the bbOA concentrations in Patras using an Aerosol Mass Spectrometer. They reported two major peaks: one during the morning and a larger one in the evening. We estimated that the nighttime emissions are four times higher than the morning ones combining these bbOA measurements and the average mixing height diurnal variation predicted by WRF for the simulated period. Also, based on the Florou et al. (2017) bbOA concentration measurements we assumed that biomass burning emissions peak at 21:00 with a decrease afterwards reaching practically zero after midnight. The assumed temporal distribution is shown in Figure 3a.

3.2.3 Day-to-day variation

$PM_{2.5}$ emissions from fireplaces are expected to vary day-to-day based on ambient temperature. They are expected to be low or even zero during the warmer days of the winter and to increase in colder days. As a zeroth order approximation we assumed that fireplaces are not used at all when the evening is warm enough. We define here the "warm enough" night as one in which the average temperature of the urban area between 17:00-24:00 LT is above 16 ^{o}C. Above 16 ^{o}C, biomass burning $PM_{2.5}$ ($bbPM_{2.5}$) emissions are assumed to be zero. Below 16 ^{o}C, $bbPM_{2.5}$ emissions are assumed to increase 6% per 1 ^{o}C (Fig. 3b). The $bbPM_{2.5}$ emissions that are estimated in

Section 3.1.1 (base case emissions) correspond to 10 °C, which is approximately the average temperature (from 17:00 to 24:00 LT) in the region during winter.

3.2.4 Volatility distribution and aging of bbOA

PMCAMx treats bbOA as semivolatile and chemically reactive. The volatility distribution of wintertime bbOA emissions applied in the model, was based on the measurements of May et al. (2013) (Fig. 3c). This volatility distribution suggests that 20% of the emitted OA has low volatility, 50% is semi-volatile and the remaining 30% consists of intermediate volatility species. This approach results in the evaporation of a significant fraction of the emissions as they are diluted in the atmosphere.

We simulate only the homogeneous oxidation of bbOA with OH assuming a rate constant equal to 4×10^{-11} cm^3 $molecule^{-1}$ s^{-1} (Atkinson and Arey, 2003). Kodros et al. (2020) suggested that the homogeneous reaction of bbOA with OH is the dominant daytime process. Nighttime reactions will be added in future applications.

3.2.5 Chemical composition of biomass burning $PM_{2.5}$

The PM_1 emitted by fireplaces and wood stoves in Greece is assumed to consist of approximately 82% OA, 16% BC (black carbon) and 2% other components based on the measurements of Kodros et al. (2022).

3.3 $PM_{2.5}$ Measurements

A low-cost sensor network that measures $PM_{2.5}$ concentrations exists in Patras (Kosmopoulos et al., 2022). Kosmopoulos et al. (2020) have evaluated the performance of the Purple Air sensors and have proposed the following correction: $PM_{2.5} = 0.42\ PAir_{2.5} + 0.26$ (μg m^{-3}), where $PM_{2.5}$ is the corrected concentrations and $PAir_{2.5}$ is the raw value. The effect of temperature and relative humidity (RH) on the measured $PM_{2.5}$ was found to be negligible for the conditions and $PM_{2.5}$ of Patras. Figure 1 shows the locations of the low-cost sensors operating in the city and its surrounding areas.

4. Results

4.1 Biomass burning organic aerosol concentration

The spatial distributions of average predicted concentrations of fresh, secondary and total bbOA for December 2021 are depicted in Figure 4. The average concentration of primary bbOA (bbPOA) in the suburban site of Kypseli is predicted to be 15 μg m^{-3}, in Agia 3.5 μg m^{-3}, while it is lower than 1 μg m^{-3} at the University of Patras (Fig. 4a). The average concentration of bbPOA for the inner modeling domain is 0.65 μg m^{-3}. PMCAMx predicts secondary bbOA (bbSOA) concentrations lower than 1 μg m^{-3} in the urban area (Fig. 4b), because most of the SOA production takes place after the biomass burning emissions have been transported away from the inner domain. Thus, more than 99% of total predicted bbOA in the urban area is primary (Fig. 4c). The effects of nighttime chemistry that can contribute to local SOA formation are neglected in this study.

The predicted hourly concentrations of fresh bbOA for three sites in Patras are shown in Figure 5. These sites include the high-density biomass burning emission area of Kypseli, the Agia site, which is located next to the city center but with lower-density housing and the background area of the University of Patras. For Kypseli, the highest bbOA hourly concentration is predicted on December 29, close to 140 μg m^{-3} (Fig. 5a). The concentrations peak mainly during the nighttime due to intense use of fireplaces for residential heating during these hours. Fresh bbOA concentrations in Agia are lower compared to Kypseli with an average concentration of 3.5 μg m^{-3} for the simulated month (Fig. 5b). The maximum hourly concentration of bbPOA is predicted on December 28 of approximately 50 μg m^{-3}. In the outskirts of the city, at the University of Patras, the bbPOA is lower, up to 12 μg m^{-3}, due to lack of important local emissions from fireplaces near this site (Fig. 5c). The concentrations in this background site are affected by transported emissions from nearby areas such as Rio. The predicted bbSOA concentrations are lower than 1 μg m^{-3} for all sites (Fig. S1).

The average predicted diurnal profiles of total bbOA concentrations for Kypseli, Agia and University are shown in Figure 6. The behavior of bbOA is similar for Kypseli and Agia. The model predicts one high peak during the nighttime at 21.00 LT and another one in the morning at 9:00 LT due to intense biomass burning activity during these hours (Fig. 6a, b). In Kypseli, the maximum average daily concentration is close to 60 μg m^{-3} at 21:00 LT (Fig. 6a). The average diurnal variation in Agia is similar to Kypseli due to the dominance of the local bbOA emissions in those sites (Fig. 6b). The maximum average concentration during the day in Agia is predicted to be 15 μg m^{-3} at 21:00 LT. At the suburbs, the bbOA concentrations are much lower, with a maximum average daily concentration close to 2 μg m^{-3} (Fig. 6c). The average diurnal profile at the University has some day and night peaks as the other sites but at much lower levels.

4.2 Predicted contribution of bbOA to OA and $PM_{2.5}$

At the suburban area of Kypseli, the predicted contribution of bbOA to total OA is 94% on average (Fig. 7a). The contribution is close to 70% in Agia and is reduced to 36% at the University of Patras. The model predicts the highest contribution in Kypseli due to high local bbOA emissions in that area, while at the background site of the University, residential biomass burning is low. During the peak bbOA level period, at 21:00 LT, the bbOA contribution increases to 97% in Kypseli, 88% in Agia and 62% at the University, indicating that biomass burning is the dominant source of air pollution during the evening (Fig. 7b). During this period, the bbOA concentration was 60 μg m^{-3} in the area of Kypseli, 14 μg m^{-3} in Agia and 2 μg m^{-3} at the University.

On average, the predicted contribution of bbOA to $PM_{2.5}$ is 80% in Kypseli, 40% in Agia and 12% at the University (Fig. S2a). During the night at 21:00 LT, the contributions rise to 92% in Kypseli, 70% in Agia and 30% at the University (Fig. S2b).

4.3 $PM_{2.5}$ predictions and model evaluation

Figure 8a depicts the average predicted $PM_{2.5}$ ground concentrations during December 2021. The highest concentration is predicted in the suburban area of Kypseli close to 20 μg m^{-3}, while at the suburbs of the city, at the University of Patras, the average concentration is much lower, 5 μg m^{-3}, 75% lower than Kypseli (Fig. 8a). In Agia, the average $PM_{2.5}$ concentration is 8 μg m^{-3}. During the period of maximum bbOA concentrations, at 21:00 LT, in Kypseli, the average predicted $PM_{2.5}$ concentration is 65 μg m^{-3}, in Agia 20 μg m^{-3}, while at the University of Patras 6.5 μg m^{-3} (Fig. 8b).

The predicted total $PM_{2.5}$ average diurnal profiles are compared against the measured ones from the corresponding low-cost sensors during the simulation period for five sites (Kypseli, Demenika, Koukouli, Agia and University of Patras) covering the various city areas (Fig. 9). Also, Figure 10 depicts the average diurnal profile of $PM_{2.5}$ source contributions predicted by the PSAT algorithm for the five sites. For Kypseli, the model reproduces well on average the measured $PM_{2.5}$ diurnal variations. The model reproduces the high nighttime peak of approximately 60 μg m^{-3} and also reproduces the morning one (Fig. 9a). Both nighttime and morning peaks are related to biomass burning activity for residential heating during these hours (Fig. 10a).

For the sites of Demenika and Koukouli, PMCAMx tends to overpredict both the nighttime and morning peaks. Despite that, the overall behavior during the day is similar to the measured one for both sites (Fig. 9b, c). Analyzing the sources of $PM_{2.5}$, biomass burning is the dominant source of fine PM during that period (Fig. 10b, c). In Agia, the model can reproduce the high peak at night, but also the morning one. Predicted and measured $PM_{2.5}$ nighttime peaks are three times lower than the ones in Kypseli. Specifically, the predicted nighttime peak is 64 μg m^{-3} in Kypseli and 21 μg m^{-3} and Agia, while the measured ones are 58 and 18 μg m^{-3}, respectively (Fig. 9d). Biomass burning for residential heating is the most important source during the nighttime (Fig. 10d).

At the outskirts of the city, at the University of Patras, PMCAMx tends to overpredict the measured $PM_{2.5}$ concentrations (Fig. 9e). Both measured and predicted $PM_{2.5}$ concentrations during the day are lower than inside the city, due to low biomass burning activity in that site. Most of $PM_{2.5}$ at the University is transported there from nearby areas, while low peaks from biomass burning are predicted at 10:00 LT in the morning and early in the night (Fig.10e). At this background site, long-range transport contributes 82% on average to $PM_{2.5}$ according to PSAT, while biomass burning is responsible for 10% of the $PM_{2.5}$ on average.

A simulation for the same period but without biomass burning emissions was also conducted. Predicted $PM_{2.5}$ concentrations without bbOA emissions have a different average diurnal profile due to lack of biomass burning OA emissions (Fig. S3). Average $PM_{2.5}$ concentrations are lower than 7 μg m^{-3} for all sites with three peaks. The peak in the early morning is related to transportation, the peak after the midday is due to cooking, while the nighttime one is related to cooking and transport.

In general, the model reproduces the measured high nighttime peaks for Kypseli and Agia, tends to overestimate the peaks in Demenika, Koukouli and the University of Patras, while it can reproduce well the overall behavior of concentrations during the day. Discrepancies between measurements and predictions are due to uncertainties in emissions estimates, meteorology and the low-cost sensor measurements.

4.3.1 *Evaluation metrics*

$PM_{2.5}$ daily measurements from the low cost-sensors were used to evaluate PMCAMx predictions as there were no bbOA AMS measurements for the simulation period. The studies of Florou et al. (2017) and Kodros et al. (2020) showed that in Patras during the winter nighttime more than 90% of the $PM_{2.5}$ is OA. Also, PMCAMx predicted that OA is the major component of $PM_{2.5}$ in the urban core (Fig. S4). We take advantage of this dominance of bbOA during the simulated nights and evaluate the model predictions against $PM_{2.5}$ observations in several locations. This evaluation reflects, at least as a first approximation, the ability of the model to simulate bbOA at least during the peak concentration periods. The mean bias (MB), mean absolute gross error (MAGE), fractional bias (FBIAS), fractional error (FERROR) and index of agreement (IOA) are calculated as: $\mathrm{MB} = 1/n\sum_{i=1}^{n}(P_i - O_i)$

$$\mathrm{MAGE} = 1/n\sum_{i=1}^{n}|P_i - O_i|$$

$$\mathrm{FBIAS} = 2/n\sum_{i=1}^{n}(P_i - O_i)\,/(P_i + O_i)$$

$$\mathrm{FERROR} = 2/n\sum_{i=1}^{n}|P_i - O_i|\,/(P_i + O_i)$$

$$\mathrm{IOA} = 1 - \sum_{I=1}^{n}(P_i - O_i)^2 \Big/ \sum_{I=1}^{n}(|P_i - \bar{O}| + |O_i - \bar{O}|)^2$$

where, P_i is the predicted daily $PM_{2.5}$ concentration, O_i is the observed $PM_{2.5}$ concentration, $\bar{O}_i$ the mean observed $PM_{2.5}$ concentration and n is the number of data points. The evaluation metrics of daily $PM_{2.5}$ measurements and predictions for several sites in Patras are shown in Table 1. For the area of high bbOA emissions, Kypseli, the FBIAS and FERROR were -0.01 and 0.3, while the mean observed and mean predicted $PM_{2.5}$ concentrations were 19.9 and 18.9 μg m^{-3} respectively. For the background area of the University, the FBIAS and FERROR were 0.24 and 0.47 and the mean observed and predicted fine PM concentrations were 3.7 and 4.8 μg m^{-3} respectively. Also, for the sites of Demenika, Koukouli, Agia and Agia Sofia, the FBIAS and FERROR was less than 25% and 50%. The PMCAMx performance of $PM_{2.5}$ on a daily scale is considered excellent (FBIAS≤±15% and FERROR≤±35%) for this application for Kypseli, while is considered good (FBIAS≤±30% and FERROR≤±50%) for Demenika, Koukouli, Agia, Agia Sofia and University based on the criteria of Morris et al. (2005).

The model performance of $PM_{2.5}$ is considered average (FBIAS≤±60% and FERROR≤±75%) for the background sites of Kastelokampos and Platani based on the same criteria. Model errors in these areas with relatively low concentrations are mainly related to errors in the fine PM levels transported to the area from other parts of Greece or Europe.

The evaluation metrics of hourly $PM_{2.5}$ predictions and observations are presented in Table 2 for several sites in Patras. Mean bias for all studied sites was lower than 2.5 μg m^{-3} and MAGE lower than 12.5 μg m^{-3}. The highest MAGE was for the high-biomass-burning-emission areas, while the lowest for the background sites due to low bbOA emissions. Fractional bias ranged from -4 to 25% and fractional error from 65 to 85%.

5. Sensitivity tests

Two additional simulations for December 2021 with double and half the bbOA emissions were performed. The predicted average concentrations of fresh and oxidized bbOA are predicted to be approximately proportional to the changes in bbOA emissions (Fig. S5, S6). For the case of doubling bbOA emissions, the average ground concentrations of fresh bbOA in Kypseli, Agia and University are predicted to be 30, 7.3 and 1.3 μg m^{-3} respectively, which are approximately double the values predicted by the base case simulation. If the bbOA emissions are reduced by 50%, the corresponding values are equal to 7.3, 1.7 and 0.3 μg m^{-3}, almost half of those of the base case (Fig. S5). Similar behavior is observed for the secondary bbOA average concentrations for both sensitivity tests (Fig. S6).

For Kypseli, the maximum daily average concentration is predicted to be 127 μg m^{-3} for double the bbOA emissions, 34 μg m^{-3} for half the emissions and 64 μg m^{-3} for the base case scenario (Fig. S7a). The changes in bbOA emissions are proportional to the changes in concentrations for this site with the highest bbOA emissions. Similar behavior is predicted for Demenika, Koukouli and Agia (Fig. S7b, c, d). At the University of Patras, the maximum daily average concentration is 6.5 μg m^{-3} for the base case, 8.6 μg m^{-3} when the emissions are doubled and 5.4 μg m^{-3} when they are halved (Fig. S7e). In this area outside the city, the changes in $PM_{2.5}$ concentrations are not proportional to bbOA emissions, because most of $PM_{2.5}$ in this background site comes from long-range transport and the local contribution of emissions is lower. When the bbOA emissions are reduced by 50%, a better agreement between predictions and measurements is observed for the sites of Koukouli and University. This suggests that may be the emissions in these areas have been overestimated.

The results of these sensitivity tests along with the corresponding deviations of PMCAMx predictions from observations can be used to estimate at least to a zeroth degree the uncertainty of the estimated bbOA emissions. This of course assumes that the bbOA emissions are the major source of error in the model predictions. Use of the base case emissions allows PMCAMx to reproduce well the measurements in the high-biomass-burning-emissions area of Kypseli and in the urban site of Agia. Emission rates lower by 50% are needed to reproduce the measurements in Koukouli and University. For Demenika, bbOA emissions lower by approximately 25% compared to the base case emissions are needed to reproduce the measurements.

6. Conclusions

Residential $PM_{2.5}$ emissions for heating purposes were estimated for the urban area of Patras of 8100 kg d^{-1} with a little more than 80% of the PM being organic. This corresponds to approximately 40 g d^{-1} per person. PMCAMx was applied over Europe focusing on the urban area of Patras to simulate the air pollution during the wintertime. The model predicted the highest bbOA concentrations in the high-density housing site of Kypseli and the lowest ones at the outskirts of the city. During the day, the highest bbOA concentrations are predicted from early in the evening until midnight, while they peak at 21.00 LT due to intense biomass burning activity these hours. The predicted daytime production of bbSOA in the urban area was small (less than 1% of the bbOA). $PM_{2.5}$ was dominated by bbOA with a contribution of 88% on average in the high-bbOA emission area. The dominant source of $PM_{2.5}$ in the urban and suburban core was the residential biomass burning, while at the suburbs of the city, long-range transport was the dominant one.

The model using the base case emissions reproduced well the $PM_{2.5}$ concentrations for the area of high bbOA emissions and the center of the city, while it tended to underestimate the $PM_{2.5}$ concentrations for the outskirts of the city. Driving variables for the discrepancies between model and measurements were uncertainties in bbOA emissions such as the number of households that use fireplaces for heating, errors in meteorology and uncertainties in the low-cost sensor measurements.

During the wintertime period, daily $PM_{2.5}$ concentrations often exceeded the 24-hour $PM_{2.5}$ WHO limit of 15 μg m^{-3} mainly due to the intense residential wood burning in fireplaces. Thus, restricting the use of fireplaces is clearly needed.

The developed methodology can be applied to other urban areas to add this important source of pollution of residential biomass burning to emission inventories and chemical transport models. Additional measurements for larger periods and model applications can be used for further reduction of the uncertainty of the bbOA emissions estimated in this work. Addition of nighttime processing would also be useful to better estimate the secondary OA product.

Acknowledgements

This work was supported by the EU H2020 Research Infrastructures Services Reinforcing Air Quality Monitoring Capacities in European Urban & Industrial AreaS (RI-URBANS) project (grant 101036245).

References

Akagi, S.K., Yokelson, R.J., Wiedinmyer, C., Alvarado, M.J., Reid, J.S., Karl, T., Crounse, J.D., and Wennberg, P.O., 2011. Emission factors for open and domestic biomass burning for use in atmospheric models. Atmos. Chem. Phys. 11, 4039–4072.

Alfarra, M.R., Prevot, A.S.H., Szidat, S., Sandradewi, J., Weimer, S., Lanz, V.A., Schreiber, D., Mohr, M., and Baltensperger, U., 2007. Identification of the mass spectral signature of organic aerosols from wood burning emissions. Environ. Sci. Technol. 41, 5770–5777.

Alves, C., Gonçalves, C., Fernandes, A.P., Tarelho, L., and Pio, C., 2011. Fireplace and woodstove fine particle emissions from combustion of western Mediterranean wood types. Atmos. Res. 101, 692–700.

Athanasopoulou, E., Speyer, O., Brunner, D., Vogel, H., Vogel, B., Mihalopoulos, N., and Gerasopoulos, E., 2017. Changes in domestic heating fuel use in Greece: Effects on atmospheric chemistry and radiation. Atmos. Chem. Phys. 17, 10597–10618.

Atkinson, R., and Arey, J., 2003. Atmospheric degradation of volatile organic compounds. Chem. Rev., 103, 4605–4638.

Burr, M.J., and Zhang, Y., 2011. Source apportionment of fine particulate matter over the Eastern U.S. Part I: Source sensitivity simulations using CMAQ with the Brute Force method. Atmos. Pollut. Res. 2, 300–317.

Cappa, C.D., and Jimenez, J.L., 2010. Quantitative estimates of the volatility of ambient organic aerosol. Atmos. Chem. Phys. 10, 5409–5424.

Carter, W.P.L., 2000. Documentation of the SAPRC-99 Chemical Mechanism for VOC Reactivity Assessment. Report to California Air Resources Board. Available online: https://intra.engr.ucr.edu/~carter/absts.htm#saprc99.
Castro, A., Calvo, A.I., Blanco-Alegre, C., Oduber, F., Alves, C., Coz, E., Amato, F., Querol, X., and Fraile, R., 2018. Impact of the wood combustion in an open fireplace on the air quality of a living room: Estimation of the respirable fraction. Sci. Total Environ. 628–629, 169–176.
Crippa, M., Canonaco, F., Slowik, J.G., El Haddad, I., Decarlo, P.F., Mohr, C., Heringa, M.F., Chirico, R., Marchand, N., Temime-Roussel, B., Abidi, E., Poulain, L., Wiedensohler, A., Baltensperger, U., and Prévôt, A.S.H., 2013a. Primary and secondary organic aerosol origin by combined gas-particle phase source apportionment. Atmos. Chem. Phys. 13, 8411–8426.
Crippa, M., DeCarlo, P.F., Slowik, J.G., Mohr, C., Heringa, M.F., Chirico, R., Poulain, L., Freutel, F., Sciare, J., Cozic, J., Di Marco, C.F., Elsasser, M., Nicolas, J.B., Marchand, N., Abidi, E., Wiedensohler, A., Drewnick, F., Schneider, J., Borrmann, S., Nemitz, E., Zimmermann, R., Jaffrezo, J.-L., Prévôt, A.S.H., and Baltensperger, U., 2013b. Wintertime aerosol chemical composition and source apportionment of the organic fraction in the metropolitan area of Paris. Atmos. Chem. Phys. 13, 961–981.
Donahue, N.M., Robinson, A.L., Stanier, C.O., and Pandis, S.N., 2006. Coupled partitioning, dilution, and chemical aging of semivolatile organics. Environ. Sci. Technol. 40, 2635–2643.
Emmons, L.K., Walters, S., Hess, P.G., Lamarque, J.-F., Pfister, G.G., Fillmore, D., Granier, C., Guenther, A., Kinnison, D., Laepple, T., Orlando, J., Tie, X., Tyndall, G., Wiedinmyer, C., Baughcum, S.L., and Kloster, S., 2010. Description and evaluation of the Model for Ozone and Related chemical Tracers, version 4 (MOZART-4). Geosci. Model Dev. 3, 43–67.
ENVIRON, 2003. User's Guide to the Comprehensive Air Quality Model with Extensions (CAMx). Version 4.02. ENVIRON International Corporation.
United States Environmental Protection Agency, 2022. Health and Environmental Effects of Particulate Matter (PM), https://www.epa.gov/pm-pollution/health-and-environmental-effects-particulate-matter-pm.
Fahey, K.M., and Pandis, S.N., 2001. Optimizing model performance: Variable size resolution in cloud chemistry modeling. Atmos. Environ. 35, 4471–4478.
Florou, K., Papanastasiou, D.K., Pikridas, M., Kaltsonoudis, C., Louvaris, E., Gkatzelis, G.I., Patoulias, D., Mihalopoulos, N., and Pandis, S.N., 2017. The contribution of wood burning and other pollution sources to wintertime organic aerosol levels in two Greek cities. Atmos. Chem. Phys. 17, 3145–3163.
Fountoukis, C., Megaritis, A.G., Skyllakou, K., Charalampidis, P.E., Pilinis, C., Denier Van Der Gon, H.A.C., Crippa, M., Canonaco, F., Mohr, C., Prévôt, A.S.H., Allan, J.D., Poulain, L., Petäjä, T., Tiitta, P., Carbone, S., Kiendler-Scharr, A., Nemitz, E., O'Dowd, C., Swietlicki, E., and Pandis, S.N., 2014. Organic aerosol concentration and composition over Europe: Insights from comparison of regional model predictions with aerosol mass spectrometer factor analysis. Atmos. Chem. Phys. 14, 9061–9076.
Fountoukis, C., Racherla, P.N., Denier Van Der Gon, H.A.C., Polymeneas, P., Charalampidis, P.E., Pilinis, C., Wiedensohler A., Dall'Osto, M., O'Dowd, C., and Pandis, S.N., 2011. Evaluation of a three-dimensional chemical transport model

(PMCAMx) in the European domain during the EUCAARI May 2008 campaign. Atmos. Chem. Phys. 11, 10331–10347.

Fuller, G.W., Sciare, J., Lutz, M., Moukhtar, S., and Wagener, S., 2013. New Directions: Time to tackle urban wood burning? Atmos. Environ. 68, 295–296.

Fuller, G.W., Tremper, A.H., Baker, T.D., Yttri, K.E., and Butterfield, D., 2014. Contribution of wood burning to PM_{10} in London. Atmos. Environ. 87, 87–94.

Gaidajis, G., Angelakoglou, K., and Aktsoglou, D., 2014. Wintertime particulate mass concentrations in urban environment and the impact of economic crisis. J. Environ. Sci. Health A 49, 1653–1660.

Gaydos, T.M., Koo, B., Pandis, S.N., and Chock, D.P., 2003. Development and application of an efficient moving sectional approach for the solution of the atmospheric aerosol condensation/evaporation equations. Atmos. Environ. 37, 3303–3316.

Gonçalves, C., Alves, C., and Pio, C., 2012. Inventory of fine particulate organic compound emissions from residential wood combustion in Portugal. Atmos. Environ. 50, 297–306. https://doi.org/10.1016/j.atmosenv.2011.12.013.

Grieshop, A.P., Miracolo, M.A., Donahue, N.M., and Robinson, A.L., 2009. Constraining the volatility distribution and gas-particle partitioning of combustion aerosols using isothermal dilution and thermodenuder measurements. Environ. Sci. Technol. 43, 4750–4756. https://doi.org/10.1021/es8032378.

Hayes, R.B., Lim, C., Zhang, Y., Cromar, K., Shao, Y., Reynolds, H.R., Silverman, D. T., Jones, R.R., Park, Y., Jerrett, M., Ahn, J., and Thurston, G.D., 2020. $PM_{2.5}$ air pollution and cause-specific cardiovascular disease mortality. Int. J. Epidemiol. 49, 25–35. https://doi.org/10.1093/ije/dyz114.

Hellenic Statistical Authority, 2011. Characteristics of dwellings-households (in Greek). https://www.statistics.gr/en/statistics/-/publication/SAM05/2011.

Hennigan, C.J., Miracolo, M.A., Engelhart, G.J., May, A.A., Presto, A.A., Lee, T., Sullivan, A.P., McMeeking, G.R., Coe, H., Wold, C.E., Hao, W.M., Gilman, J.B., Kuster, W.C., De Gouw, J., Schichtel, B.A., Collett, J.L., Kreidenweis, S.M., and Robinson, A.L., 2011. Chemical and physical transformations of organic aerosol from the photo-oxidation of open biomass burning emissions in an environmental chamber. Atmos. Chem. Phys. 11, 7669–7686. https://doi.org/10.5194/acp-11-7669-2011.

Hu, Y., Balachandran, S., Pachon, J.E., Baek, J., Ivey, C., Holmes, H., Odman, M.T., Mulholland, J.A., and Russell, A.G., 2014. Fine particulate matter source apportionment using a hybrid chemical transport and receptor model approach. Atmos. Chem. Phys. 14, 5415–5431. https://doi.org/10.5194/acp-14-5415-2014.

Kalogridis, A.C., Vratolis, S., Liakakou, E., Gerasopoulos, E., Mihalopoulos, N., and Eleftheriadis, K., 2018. Assessment of wood burning versus fossil fuel contribution to wintertime black carbon and carbon monoxide concentrations in Athens, Greece. Atmos. Chem. Phys. 18, 10219–10236.

Kanakidou, M., Seinfeld, J.H., Pandis, S.N., Barnes, I., Dentener, F.J., Facchini, M.C., Van Dingenen, R., Ervens, B., Nenes, A., Nielsen, C.J., Swietlicki, E., Putaud, J.P., Balkanski, Y., Fuzzi, S., Horth, J., Moortgat, G.K., Winterhalter, R., Myhre, C.E.L., Tsigaridis, K., Vignati, E., Stephanou, E.G., and Wilson, J., 2005. Organic aerosol and global climate modelling: A review. Atmos. Chem. Phys. 5, 1053–1123. https://doi.org/10.5194/acp-5-1053-2005.

Kodros, J.K., Kaltsonoudis, C., Paglione, M., Florou, K., Jorga, S., Vasilakopoulou, C., Cirtog, M., Cazaunau, M., Picquet-Varrault, B., Nenes, A., and Pandis, S.N., 2022.

Secondary aerosol formation during the dark oxidation of biomass burning emissions. Environ. Sci. Atmos. 2, 1221-1236.

Kodros, J.K., Papanastasiou, D.K., Paglione, M., Masiol, M., Squizzato, S., Florou, K., Skyllakou, K., Kaltsonoudis, C., Nenes, A., and Pandis, S.N., 2020. Rapid dark aging of biomass burning as an overlooked source of oxidized organic aerosol. PNAS 117, 33028–33. https://doi.org/10.1073/PNAS.2010365117.

Kosmopoulos, G., Salamalikis, V., Matrali, A., Pandis, S.N., and Kazantzidis, A., 2022. Insights about the sources of $PM_{2.5}$ in an urban area from measurements of a low-cost sensor network. Atmosphere 13, 440.

Kosmopoulos, G., Salamalikis, V., Pandis, S.N., Yannopoulos, P., Bloutsos, A.A., and Kazantzidis, A., 2020. Low-cost sensors for measuring airborne particulate matter: Field evaluation and calibration at a South-Eastern European site. Sci. Total Environ. 748, 141396. https://doi.org/10.1016/j.scitotenv.2020.141396.

Kostenidou, E., Kaltsonoudis, C., Tsiflikiotou, M., Louvaris, E., Russell, L.M., and Pandis, S.N., 2013. Burning of olive tree branches: A major organic aerosol source in the Mediterranean. Atmos. Chem. Phys. 13, 8797–8811.

Lipsky, E.M., and Robinson, A.L., 2006. Effects of dilution on fine particle mass and partitioning of semivolatile organics in diesel exhaust and wood smoke. Environ. Sci. Technol. 40, 155–162. https://doi.org/10.1021/es050319p.

May, A.A., Lee, T., McMeeking, G.R., Akagi, S., Sullivan, A.P., Urbanski, S., Yokelson, R.J., and Kreidenweis, S.M., 2015. Observations and analysis of organic aerosol evolution in some prescribed fire smoke plumes. Atmos. Chem. Phys. 15, 6323–6335. https://doi.org/10.5194/acp-15-6323-2015.

May, A.A., Levin, E.J.T., Hennigan, C.J., Riipinen, I., Lee, T., Collett, J.L., Jimenez, J.L., Kreidenweis, S.M., and Robinson, A.L., 2013. Gas-particle partitioning of primary organic aerosol emissions: 3. Biomass burning. J. Geophys. Res. Atmos. 118, 11327-11338. https://doi.org/10.1002/jgrd.50828.

Morris, R.E., Mc Nally, D.E., Tesche, T.W., Tonnesen, G., Boylan, J.W., and Brewer, P., 2005. Preliminary evaluation of the Community Multiscale Air Quality model for 2002 over the southeastern United States. J. Air Waste Manag. Assoc. 55, 1694–1708. https://doi.org/10.1080/10473289.2005.10464765.

Murphy, B.N., Donahue, N.M., Robinson, A.L., and Pandis, S.N., 2014. A naming convention for atmospheric organic aerosol. Atmos. Chem. Phys. 14, 5825–5839. https://doi.org/10.5194/acp-14-5825-2014.

Nenes, A., Pandis, S.N., and Pilinis, C., 1999. Continued development and testing of a new thermodynamic aerosol module for urban and regional air quality models. Atmos. Environ. 33, 1553–1560. https://doi.org/10.1016/S1352-2310(98)00352-5.

Nenes, A., Pilinis, C., and Pandis., S.N., 1998. ISORROPIA: A new thermodynamic model for multiphase multicomponent inorganic aerosols. Aquat. Geochem. 4, 123–152.

Papada, L., and Kaliampakos, D., 2017. Energy poverty in Greek mountainous areas: a comparative study. J. Mt. Sci. 14, 1229-1240.

Pikridas, M., Tasoglou, A., Florou, K., and Pandis, S.N., 2013. Characterization of the origin of fine particulate matter in a medium size urban area in the Mediterranean. Atmos. Environ. 80, 264–274. https://doi.org/10.1016/j.atmosenv.2013.07.070.

Puxbaum, H., Caseiro, A., Sánchez-Ochoa, A., Kasper-Giebl, A., Claeys, M., Gelencsér, A., Legrand, M., Preunkert, S., and Pio, C.A., 2007. Levoglucosan levels at background sites in Europe for assessing the impact of biomass

combustion on the European aerosol background. J. Geophys. Res. 112, D23S05. https://doi.org/10.1029/2006JD008114.
Seinfeld, J.H., and Pandis, S.N., 2006. Atmospheric Chemistry and Physics: From Air Pollution to Climate Change. John Wiley and Sons, Hoboken, New Jersey.
Sindosi O.A., Markozannes G., Rizos E., and Ntzani E., 2019. Effects of economic crisis on air quality in Ioannina, Greece. J. Environ. Sci. Health A 54, 768-781.
Siouti, E., Skyllakou, K., Kioutsioukis, I., Ciarelli, G., and Pandis, S.N., 2021. Simulation of the cooking organic aerosol concentration variability in an urban area. Atmos. Environ. 265, 118710.
Siouti, E., Skyllakou, K., Kioutsioukis, I., Patoulias, D., Fouskas, G., and Pandis, S.N., 2022. Development and application of the SmartAQ high-resolution air quality and source apportionment forecasting system for European urban areas. Atmosphere 13, 1–20. https://doi.org/10.3390/atmos13101693.
Skamarock, W.C., Klemp, J.B., Dudhia, J., Gill, D.O., Barker, D.M., Duda, M.G., Huang, X.-Y., Wang, W., and Powers, J.G., 2008. A description of the advanced research WRF version 3. NCAR Technical Note, NCAR/TN-475+STR.
Skyllakou, K., Fountoukis, C., Charalampidis, P., and Pandis, S.N., 2017. Volatility-resolved source apportionment of primary and secondary organic aerosol over Europe. Atmos. Environ. 167, 1–10.
Slinn, S.A., and Slinn, W.G.N., 1980. Predictions for particle deposition on natural waters. Atmos. Environ. 14, 1013–1016. https://doi.org/10.1016/0004-6981(80)90032-3.
Sornek, K., Filipowicz, M., and Rzepka, K., 2017. Study of clean combustion of wood in a stove-fireplace with accumulation. J. Energy Inst. 90, 613–623. https://doi.org/10.1016/j.joei.2016.05.001.
Tambour, Y., and Seinfeld, J.H., 1980. Solution of the discrete coagulation equation. J. Colloid Inter. Sci., 74, 260–272.
Theodoritsi, G.N., and Pandis, S.N., 2019. Simulation of the chemical evolution of biomass burning organic aerosol. Atmos. Chem. Phys. 19, 5403–5415. https://doi.org/10.5194/acp-19-5403-2019.
Tian, Di, Hu, Y., Wang, Y., Boylan, J.W., Zheng, M., Russel, A.G., 2009. Assessment of biomass burning emissions and their impacts on urban and regional $PM_{2.5}$: A Georgia case study. Environ. Sci. Technol. 43, 299–305.
Vu, B., Alves, C.A., Gonçalves, C., Pio, C., Gonçalves, F., and Pereira, R., 2012. Mutagenicity assessment of aerosols in emissions from wood combustion in Portugal. Environ. Pollut. 166, 172–181.
Wesely, M.L., 2007. Parameterization of surface resistances to gaseous dry deposition in regional-scale numerical models. Atmos. Environ. 41, 52–63.
Xing, X., Zhou, Y., Lang, J., Chen, D., Cheng, S., Han, L., Huang, D., and Zhang, Y., 2018. Spatiotemporal variation of domestic biomass burning emissions in rural China based on a new estimation of fuel consumption. Sci. Total Environ. 626, 274–286. https://doi.org/10.1016/j.scitotenv.2018.01.048.
Xing, Y.F., Xu, Y.H., Shi, M.H., and Lian, Y.X., 2016. The impact of $PM_{2.5}$ on the human respiratory system. J. Thorac. Dis. 8, E69–E74.

Table 1. Metrics for daily $PM_{2.5}$ predictions during December 2021.

Site	Mean Observed (μg m^{-3})	Mean Predicted (μg m^{-3})	MB (μg m^{-3})	MAGE (μg m^{-3})	FBIAS	FERROR	IOA
Kypseli	19.9	18.9	-1.1	5.4	-0.01	0.3	0.74
Demenika	15.7	15.7	0.05	7.8	-0.17	0.49	0.71
Koukouli	10.5	13.6	3	5.8	0.25	0.5	0.54
Agia	7.8	8.1	0.36	3.7	0.05	0.5	0.5
University of Patras	3.7	4.8	1.1	1.9	0.24	0.47	0.60
Kastelokampos	8.5	5.5	-3.1	4	-0.45	0.56	0.48
Platani	5.3	4.5	-0.8	3	-0.15	0.63	0.32
Agia Sofia	11.7	9.2	-2.5	5.6	-0.2	0.5	0.32

Table 2. Metrics for hourly $PM_{2.5}$ predictions during December 2021.

Site	MB ($\mu g\ m^{-3}$)	MAGE ($\mu g\ m^{-3}$)	FBIAS	FERROR
Kypseli	-2.2	12.5	-0.12	0.65
Demenika	-0.38	12.3	-0.25	0.74
Koukouli	2.4	9.9	0.12	0.75
Agia	0.46	5.8	0.12	0.67
University of Patras	1	2.9	0.22	0.66
Kastelokampos	-3.2	5.4	-0.24	0.69
Platani	-0.9	4.3	-0.04	0.85
Agia Sofia	-3.16	8	-0.18	0.7

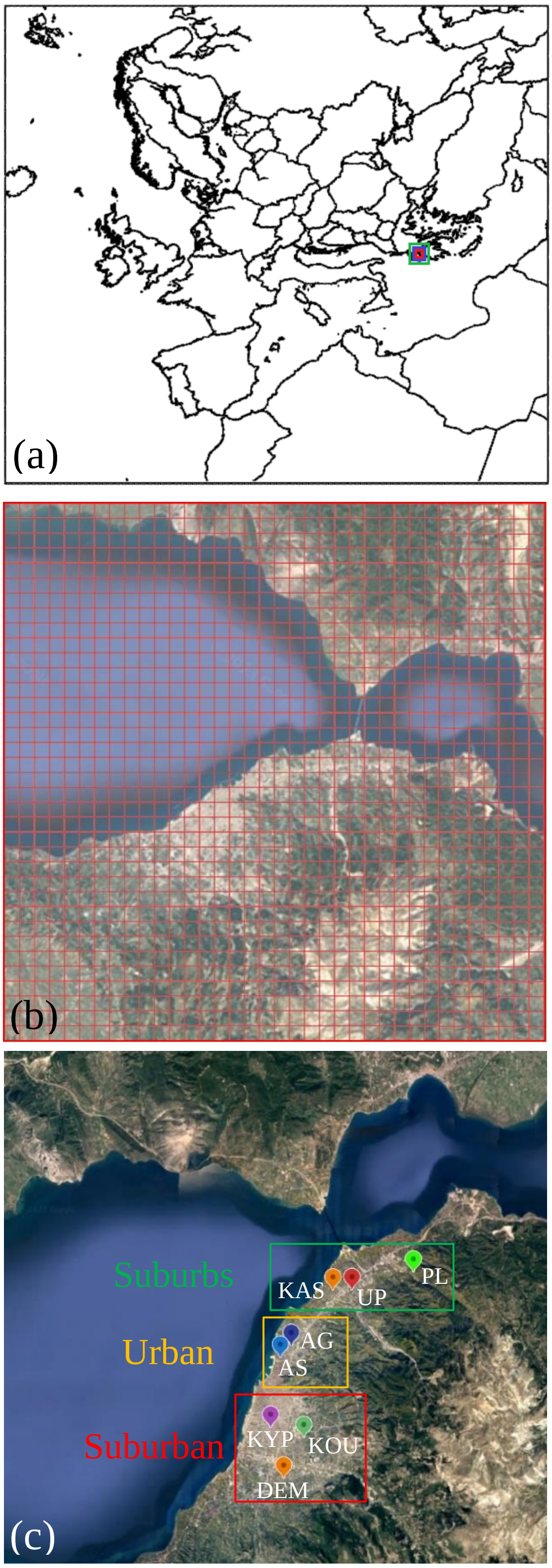

Figure 1. PMCAMx model simulation domains used in this work: (a) the outer domain of Europe with 36x36 km^2 spatial resolution and the nested domains with increasing spatial resolution, 12x12 (green), 3x3 (blue) and 1x1 (red) km^2, (b) the urban domain of Patras with 1x1 km^2 resolution and (c) the location of low-cost $PM_{2.5}$ sensors used in this study. KYP: Kypseli, DEM: Demenika, KOU: Koukouli, AG: Agia, AS: Agia Sofia, KAS: Kastelokampos, UP: University of Patras and PL: Platani.

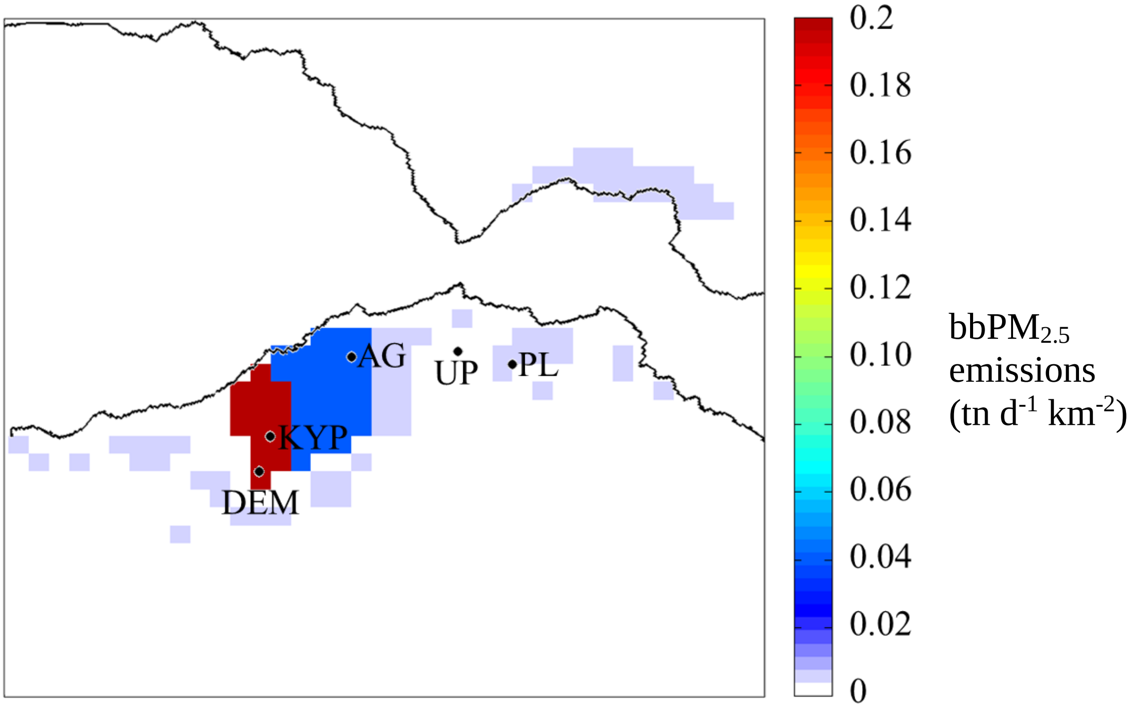

Figure 2. Estimated average primary $bbPM_{2.5}$ emissions (tn d^{-1} km^{-2}) for the urban area of Patras and its surroundings.

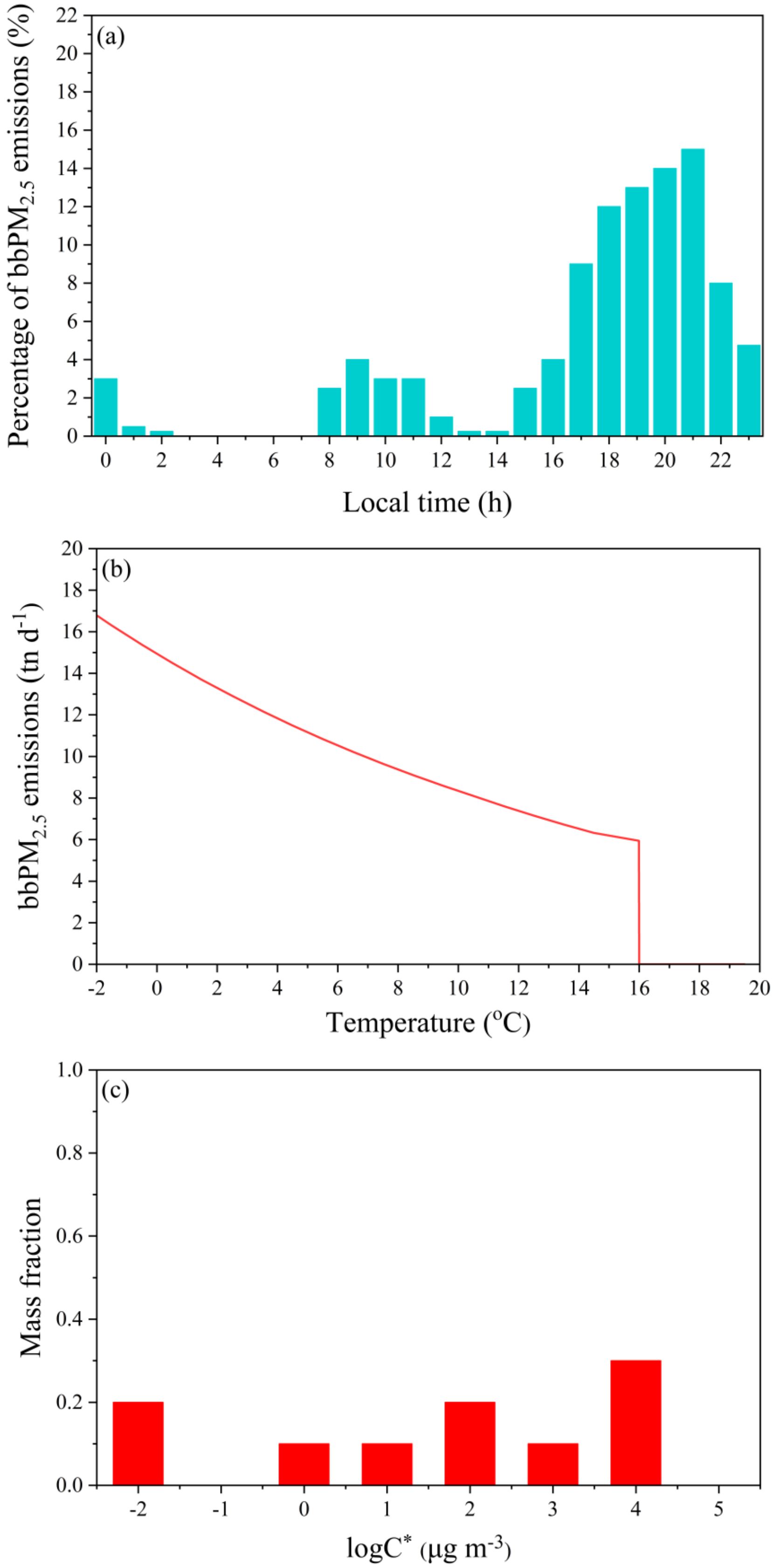

Figure 3. (a) Temporal, (b) temperature and (c) volatility distribution of $bbPM_{2.5}$ emissions.

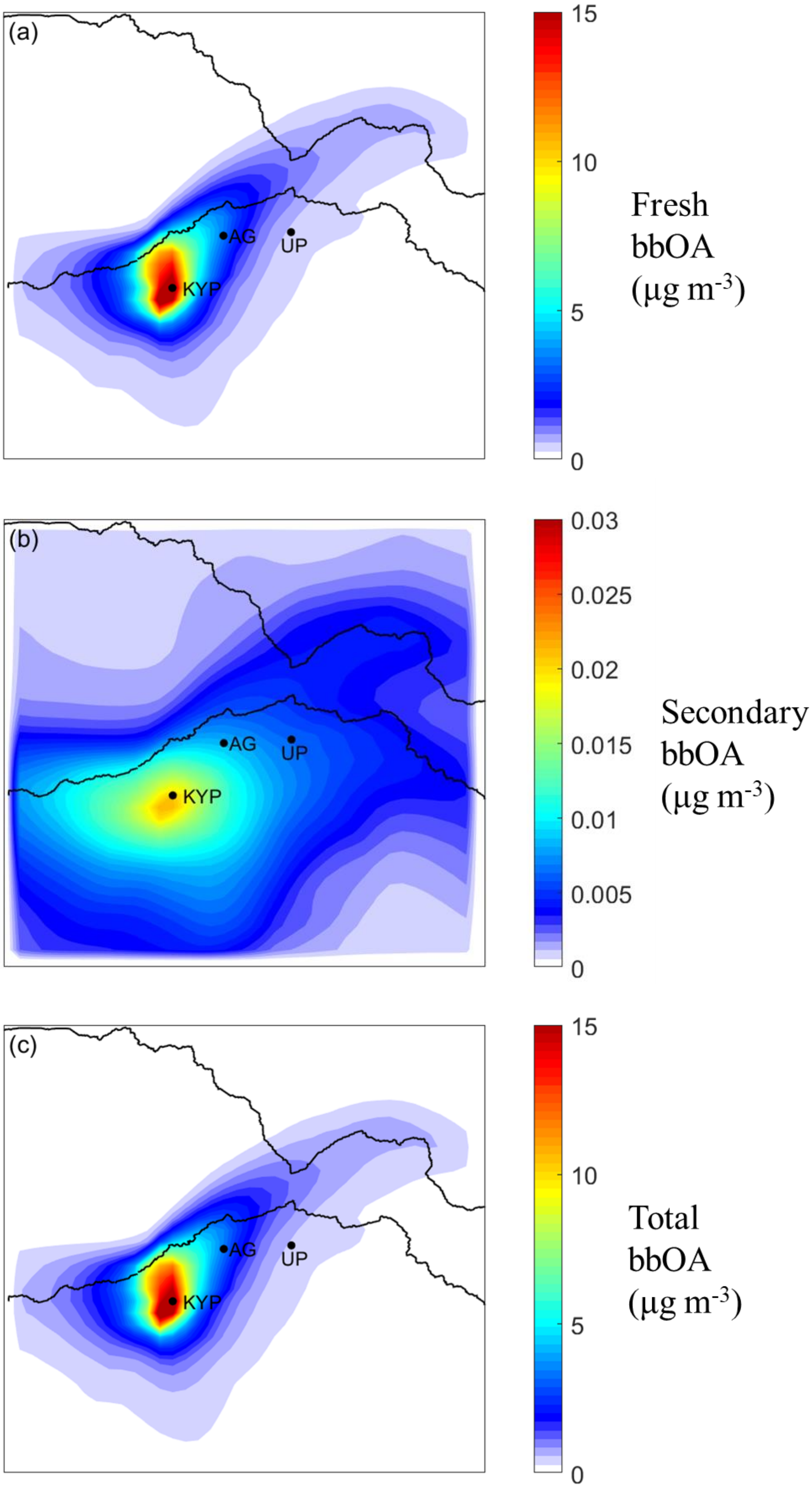

Figure 4. Predicted average ground concentrations of (a) fresh, (b) secondary and (c) total bbOA. The locations of some measurement sites are also shown. Different scales are used.

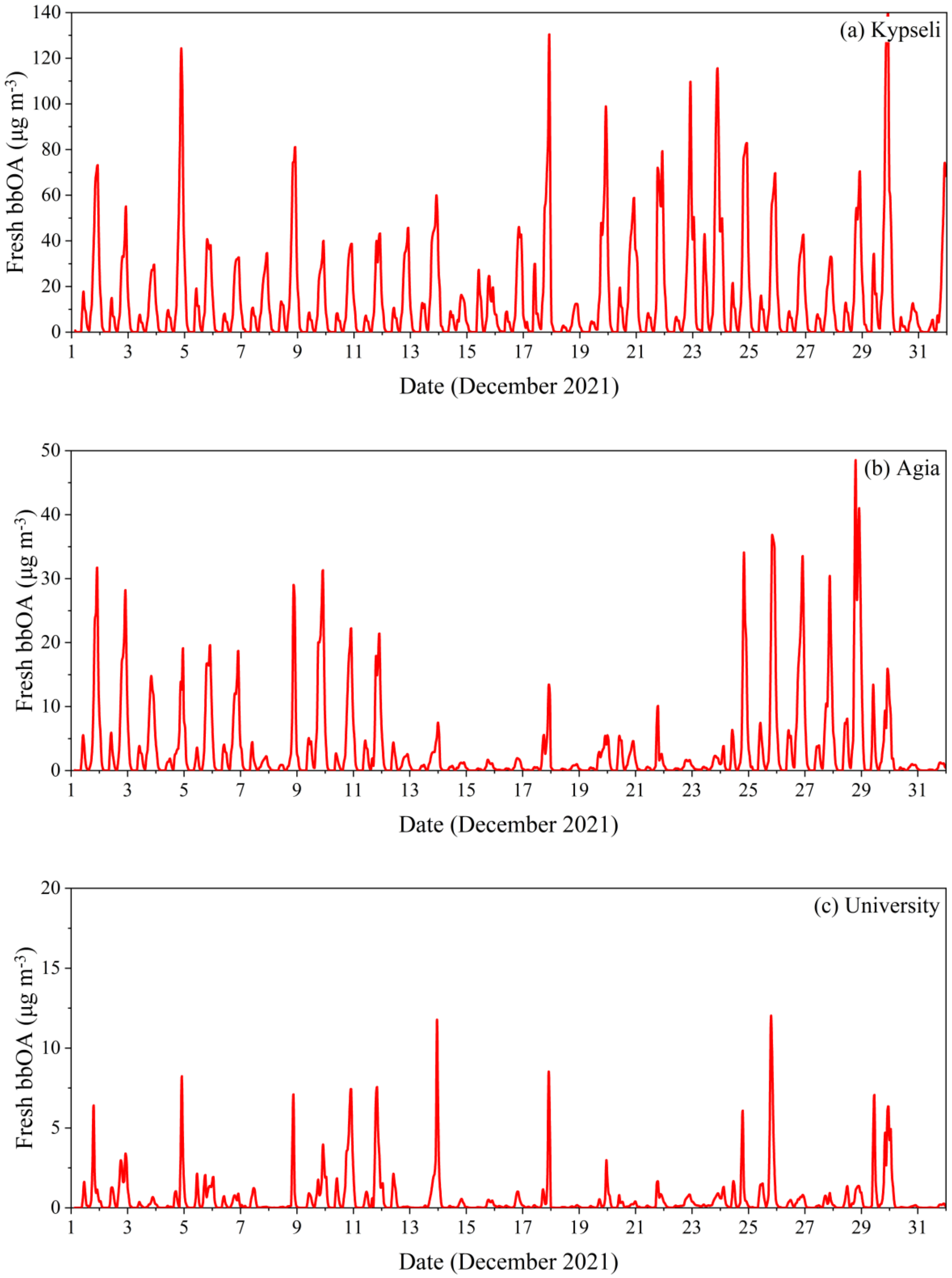

Figure 5. Predicted timeseries of fresh bbOA (μg m^{-3}) for (a) Kypseli, (b) Agia and (c) University of Patras during December 2021. Different scales are used.

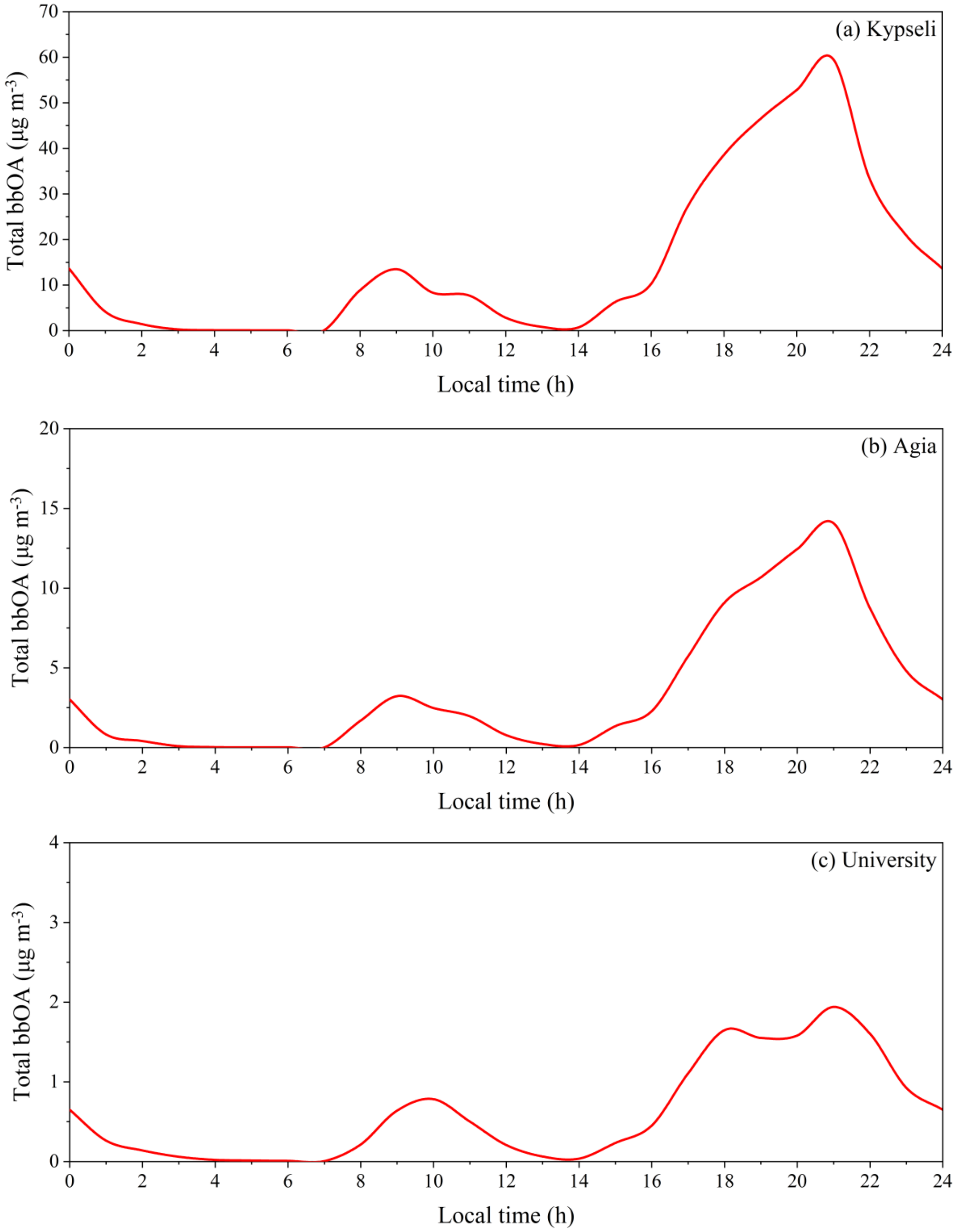

Figure 6. Predicted average diurnal profiles of total bbOA (μg m^{-3}) for (a) Kypseli, (b) Agia and (c) University of Patras during December 2021. Different scales are used.

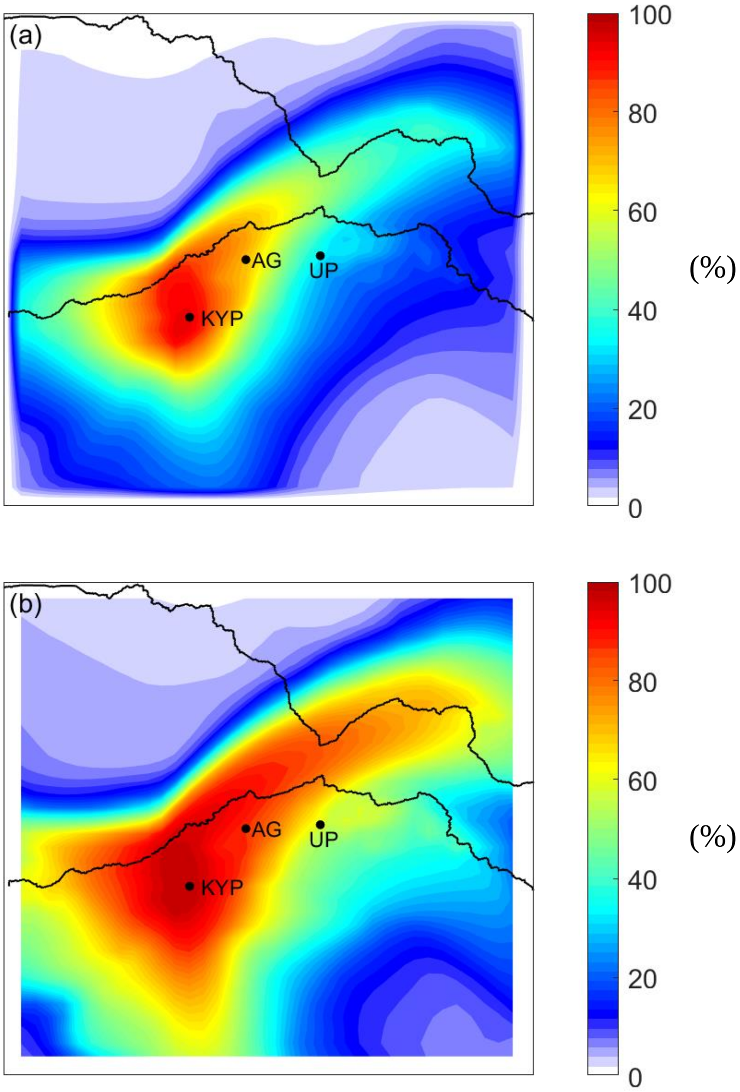

Figure 7. Contribution (%) of bbOA to total OA (a) on average and (b) at 21:00 LT during December 2021. The locations of three of the measurement sites are also shown.

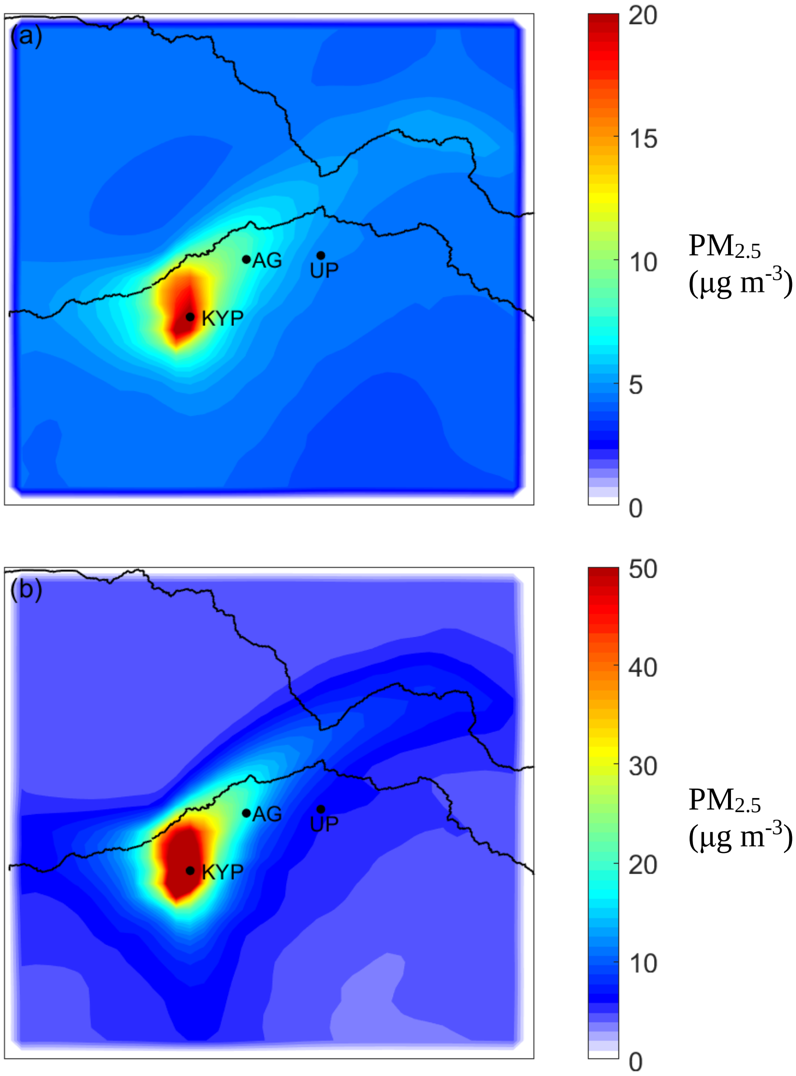

Figure 8. Predicted average ground $PM_{2.5}$ concentrations (μg m^{-3}) (a) on average and (b) at 21:00 LT during December 2021. The locations of the measurement sites are also shown. Different scales are used.

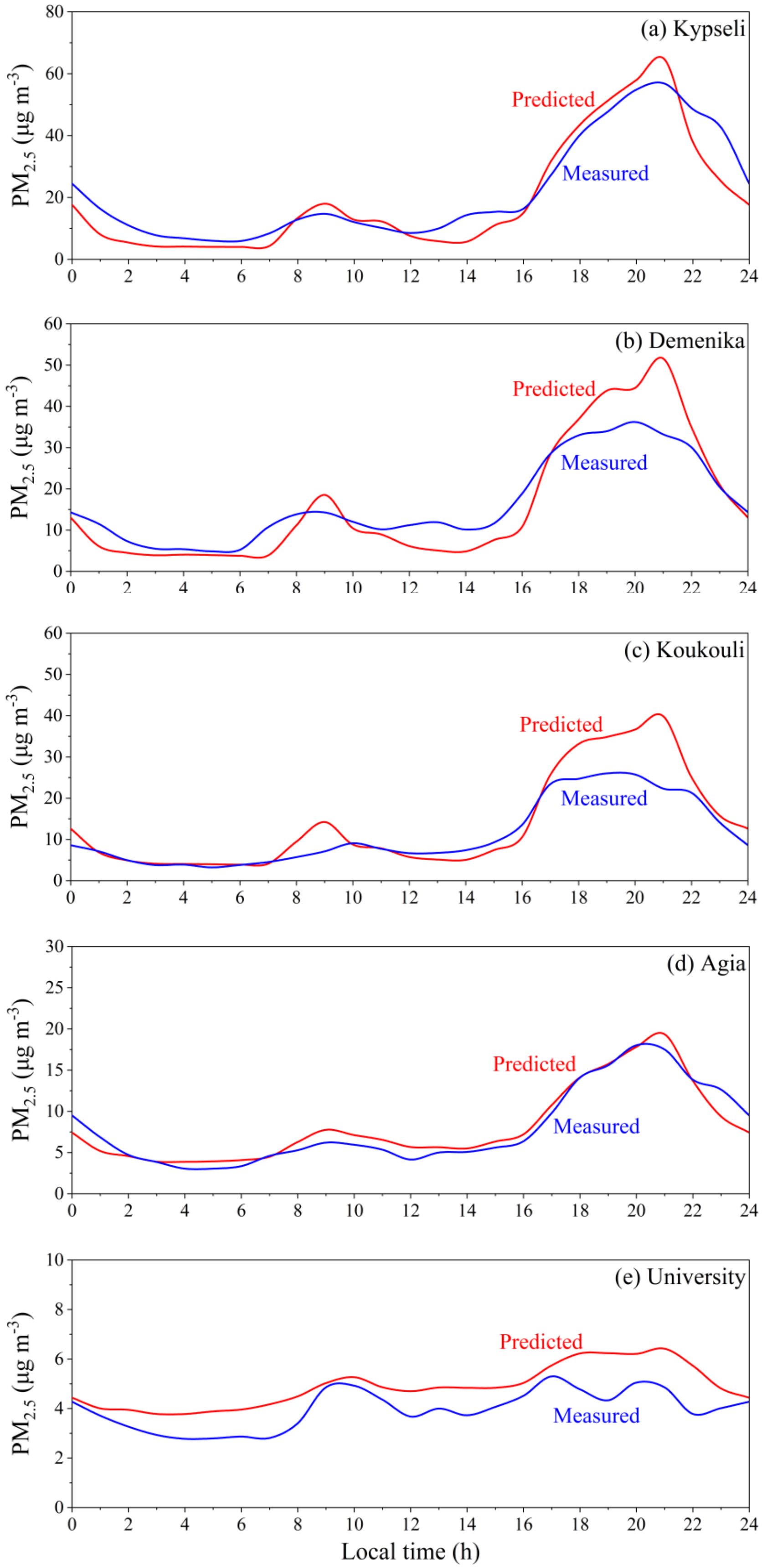

Figure 9. Predicted (with bbOA) and measured $PM_{2.5}$ average diurnal profile (μg m^{-3}) for (a) Kypseli, (b) Demenika, (c) Koukouli, (d) Agia and (c) University of Patras during December 2021. Different scales are used.

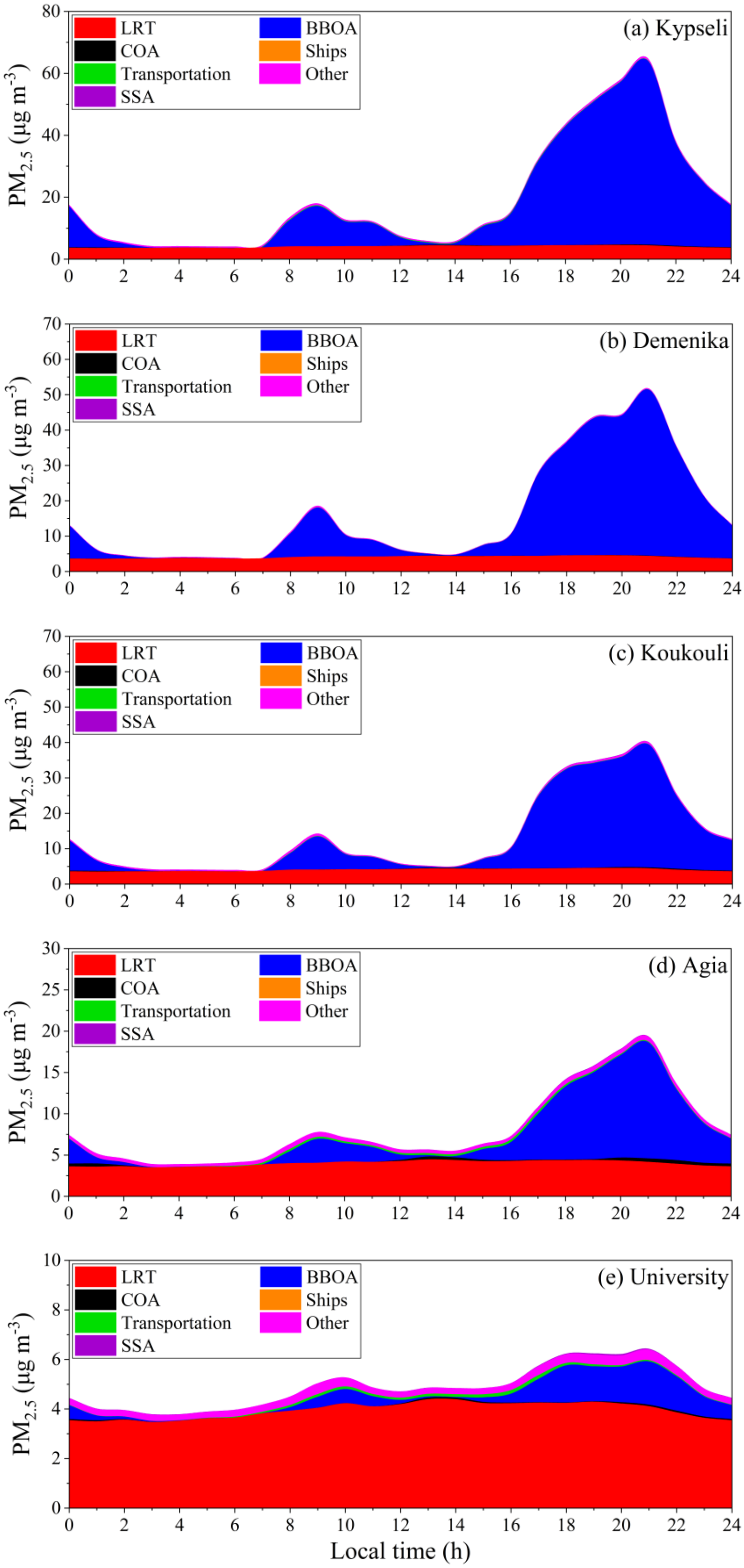

Figure 10. Predicted average diurnal profiles for $PM_{2.5}$ sources for (a) Kypseli, (b) Demenika, (c) Koukouli, (d) Agia and (c) University of Patras during the simulation period. Different scales are used.